



On the improved adhesion of NiTi wires embedded in polyester and vinylester resins

Mattia Merlin, Martina Scoponi, Chiara Soffritti, Annalisa Fortini, Raffaella Rizzoni, Gian Luca Garagnani

Department of Engineering, University of Ferrara, Via Saragat 1, I-44122 Ferrara, Italy

mattia.merlin@unife.it, martina.scoponi@unife.it, chiara.soffritti@unife.it, annalisa.fortini@unife.it, raffaella.rizzoni@unife.it, gian.luca.garagnani@unife.it

ABSTRACT. This paper discusses the effect of different surface treatments on shape memory alloy wires embedded in PolyEster (PE) and VinylEster (VE) polymeric matrices. In particular, two types of chemical etching and a chemical bonding with a silane coupling agent have been performed on the surfaces of the wires. Pull-out tests have been carried out on samples made from a specifically designed Teflon mould. Considering the best results of the pull-out tests obtained with PE resin, the debonding induced by strain recovery of 4%, 5% and 6% pre-strained NiTi wires has been evaluated with the wires being subjected to different surface treatment conditions and then being embedded in the PE matrix. The results prove that the wires functionalised and embedded in the PE resin show the maximum pull-out forces and the highest interfacial adhesion. Finally, it has been found that debonding induced by strain recovery is strongly related to the propagation towards the radial direction of sharp cracks at the debonding region.

KEYWORDS. Smart materials; Surface treatments; Thermosetting resin; Adhesion.

INTRODUCTION

Shape memory alloys (SMAs) are a class of materials with the unique characteristics of Shape Memory Effect (SME) and Superelasticity (SE), according to the temperature range and applied load. These properties are due to a crystalline, diffusionless and reversible phase transformation between the phase stable at high temperature (austenite) and the phase stable at low temperature (martensite). The shape memory effect is the ability of the alloy to recover a mechanically induced strain when heated above a critical temperature. For such alloys the knowledge of the four transformation temperatures is fundamental: M_s and M_f are the initial and final temperatures of the direct martensitic transformation from austenite to martensite on cooling, while A_s and A_f are the initial and the final temperatures of the inverse martensitic transformation from martensite to austenite on heating [1].

The specific functional properties of SMAs have been widely used to realise actuators, sensors, damping systems and devices employed in biomedical applications [2-5]. The ability of these materials to generate large recovery stresses when thermally activated has been recently used for the development of functional structures or composites, in which SMA elements are embedded in a polymeric matrix [6-10]. Several authors have proposed polymer-composite actuators with SMA strips or wires embedded in different polymeric matrices in order to improve mechanical and failure behaviour, fatigue resistance and functionality [11-15]. In particular, Thairi et al. [16] and Winzek et al. [17] studied the difference



between the phase transition temperature of the SMA and the glass transition temperature of the polymer. Barrett [18] developed a low stiffness active composite in which SMA filaments are embedded in a silicone matrix to be used for biomedical, surgical and prosthetic applications.

According to the specific application, the choice of the suitable matrix and the chemical composition of the shape memory alloy are of great importance. Functional composites, also called smart composites, take advantage of the adhesion between the active elements, in the form of SMA wires or thin strips, and the matrix. In literature, many works deal with the transformational behaviour of pre-strained NiTi wires in the martensitic phase (at $T < M_s$) embedded in a polymeric matrix. The mechanical properties of smart composites strongly depend on the efficiency of stress and strain transfer at the interface between the wires and the surrounding matrix. A great number of analytical, numerical and experimental studies of SMA fibre reinforced composites have been conducted. James and Lagoudas [19] evaluated the thermo-mechanical response of SMA hybrid composites subjected to combine thermal and mechanical loads using a finite element method. Wang and Hu [20] studied the stress transfer for an SMA fibre embedded in an elastic matrix by means of pull-out tests. Alternative theoretical methods extensively used to analyse the stress transfer in a single fibre reinforced composite are based on the shear-lag model. Liu et al. [21] found that the shear stress in the matrix and Poisson's ratio significantly influence the stress transfer between the fibre and matrix. Hsueh [22] also indicated that the radial stress and Poisson's ratio cannot be ignored when investigating stress distribution in composite materials. Wang et al. [23, 24] have developed a new theoretical model incorporating Brinson's constitutive law of SMAs for the prediction of internal stress, based on the principle of minimum complementary energy. The authors demonstrated that the new model is more general and reasonable than the classic shear-lag model. The obtained results highlighted a substantial variation in the stress distribution profile for different activation and loading conditions. Moreover, the maximum interfacial shear was located near the ends of the composite; the maximum axial stress on the fibre appeared at the midpoint of the fibre embedded length.

It is well known that the performance of SMA fibres is strongly affected by a weak fibre-matrix interfacial adhesion. In this way, adhesion quality must be improved in order to avoid degradation or premature failure of the actuation response. Over the years, laser, excimer laser and laser gas nitriding treatments have been employed [25-30]. The melting process induced by the laser treatments allows for better homogenisation of the morphology and composition of the surface. Recent works have highlighted that an improvement in interfacial adhesion can be achieved through mechanical abrasion and chemical passivation, obtained by acid solutions of the surfaces of the SMA wires [31, 32]. Both these methods increase the superficial roughness of the active elements. The chemical etching produces oxide layers that lead to a reduction in the alloy volume that displays the shape memory effect. Moreover, failure could occur at the interface between the oxide layers and the polymeric matrix. Interesting treatment methods to improve surface properties of NiTi alloys are plasma immersion and ion implantation [33, 34]. Mechanical polishing followed by a plasma treatment and then the application of a coupling agent followed by a second plasma treatment are able to realise good adhesion between a NiTi wire and an epoxy matrix [35]. Smith et al. [36] proposed functionalising the surface of the NiTi wires by using silane coupling agents. An improvement of roughly 100% in adhesion was realised as compared to untreated samples or samples functionalised with an unreactive silane coupling agent.

Several test methods, such as push-out and fragmentation tests have been developed to characterise the wire-matrix interface. However, an important test method widely used to investigate interfacial adhesion quality, interfacial properties and elastic stress transfer between fibres and matrix is the pull-out test [37, 38]. It should be noted that shear stress is related to the position in the embedded length and the debonding starts before the force reaches the maximum value [39]. Poon et al. [40] investigated the interfacial bonding behaviour of SMA composites using the fracture mechanics theory and considering the conditions of external loading acting on the SMA fibre. The SEM observations performed by Lau et al. [13] showed that failure occurred when the pre-strain in the SMA fibre and the actuation temperature are sufficiently high. Damage was preferentially localised at the fibre embedded end.

The goal of this paper is to investigate the performance of different surface treatments carried out on NiTi shape memory wires embedded in two polymeric matrices in order to improve interfacial adhesion. In particular, chemical etching by acid solutions and chemical bonding with a silane coupling agent have been evaluated. The matrices have been chosen from thermosetting resins: PolyEster and VinylEster resins. Specific pull-out samples have been realised and tested in order to compare the quality of the different surface treatments performed on wires embedded in the polymeric matrices. Based on the best results of pull-out tests, the debonding induced by the strain recovery of NiTi wires has been evaluated with the wires being subjected to different surface treatment conditions and embedded in the PolyEster resin.

The experimental characterisation aims to verify whether the increase in interfacial adhesion due to the modification of the alloy of the surface may be tailored for the design of hybrid composite devices.



MATERIALS AND METHODS

Materials

A commercially available Ti-50.7at% NiTi alloy wire of 0.5 mm in diameter has been used. Several wires of 100 mm in length have been heated at $A_f + 50^\circ\text{C}$ for 20 minutes in a furnace with an uncontrolled atmosphere and then cooled in air, in order to recover the wires initial pre-strain. After heating, the transformation temperatures (TTRs) and the latent heats per unit mass of the alloy have been evaluated by the Differential Scanning Calorimetry (DSC) technique. The DSC sample has been heated and cooled at a constant rate of $10^\circ\text{C}/\text{min}$ in the range of the martensite-austenite phase changes. The TTRs have been calculated by means of the tangent method (ASTM F2004) and the main results are collected in Tab. 1.

M_f [$^\circ\text{C}$]	M_s [$^\circ\text{C}$]	A_s [$^\circ\text{C}$]	A_f [$^\circ\text{C}$]	ΔH_M [J/g]	ΔH_A [J/g]
60.00	75.70	93.67	112.00	26.83	26.19

Table 1: Transformation temperatures and latent heats per unit mass of the NiTi wire.

The wires have been subjected to three different surface treatments, as explained in the following paragraph, and then embedded in the two thermosetting PolyEster (PE) with a 30%-Styrene content and VinylEster (VE) commercial resins. The resins need to be cured to complete the polymerisation and to give the suitable mechanical properties. The NiTi wires must be embedded in the resins before the curing heat treatment. In order to avoid the phase transformation of the NiTi alloy, a cure temperature lower than the A_s temperature should be chosen. Accordingly, samples in PE and VE resins have been cured at 90°C for 2 h and the glass transition temperature (T_g) of the post-cured resins have been evaluated through DSC measurements. The collected T_g values are 127°C and 114°C for PE and VE resin, respectively.

Surface treatments

Different surface treatments have been performed on the NiTi wires without removing the external oxide layer. The first one, called A, corresponds to a chemical etching in a 40% HNO_3 water solution for 30 min, whereas the second treatment, called AB, is a chemical etching in a 5% HNO_3 + 15% HF water solution for 20 s. Finally, the third one, called S, is the immersion in a polydimethylsiloxane coupling agent for 2 h. These three surface treatments have been compared with the wire, called NT, just heated to recover the initial pre-strain and subsequently cleaned in a methanol solution. The different analysed surface conditions are summarised in Tab. 2. Finally, the morphology of the surface of the wires has been observed and analysed by a ZEISS EVO MA15 Scanning Electron Microscope (SEM) equipped with an Energy Dispersive Spectroscopy (EDS) microprobe.

Surface treatment	Description
NT	No surface treatment
A	Chemical etching in a 40% HNO_3 water solution for 30 min
AB	Chemical etching in a 5% HNO_3 + 15% HF water solution for 20 s
S	Immersion in a polydimethylsiloxane coupling agent for 2 h

Table 2: Summary of the surface treatments.

Pull-out tests

Pull-out tests have been carried out in order to evaluate the interfacial adhesion between the two polymeric matrices and the NiTi wires in the different surface conditions. The dimensions of the pull-out samples are depicted in Fig. 1a; in particular, for each sample the wire has been embedded in a 20 mm high cylindrical specimen with a diameter of 10 mm.

As can be noted in Fig. 1b, a specific cylindrical Teflon mould, which consists of three parts, has been designed in order to realise the pull-out samples. A polymeric wax has been applied on the internal walls of the mould to prevent the resin from sticking during polymerisation and to allow the samples to be extracted.

The pull-out tests have been carried out by means of an INSTRON 4467 tensile machine with a speed rate of 1 mm/min at room temperature. The gauge length of the wire during the pull-out tests was 70 mm.

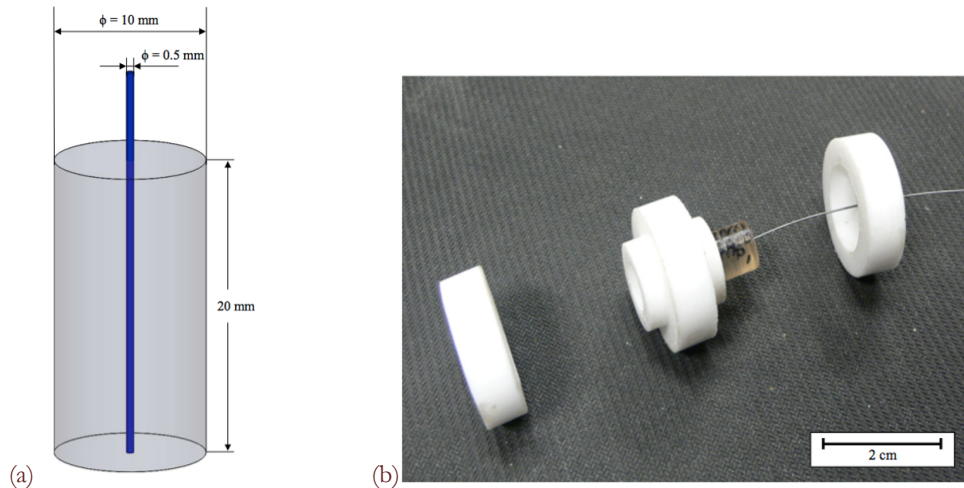


Figure 1: (a) Schematic view of the polymeric cylinder with an embedded SMA wire; (b) designed Teflon mould and pull-out sample.

Strain recovery tests

Considering the best results of the pull-out tests obtained with the PE resin, three wires for each surface treatment condition have been pre-strained by the INSTRON 4467 tensile machine at 4%, 5% and 6%, respectively. Then the pre-strained wires have been embedded in the PE resin by means of the same procedure employed for the pull-out samples. In order to achieve a statistically significant sampling, each polymeric cylinder has been transversely sectioned into discs by means of a micro cutting-off machine. The wheel speed of 3000 rpm has been selected to avoid the degradation of the polymer/wire interfaces and to prevent the wire from overheating up to the A_s transformation temperature. Five specimens of 2 mm in thickness for each surface treatment condition and pre-strained level have been obtained.

The samples have been placed into an oven for 10 min at the temperature of 120 °C, which is slightly higher than the A_f transformation temperature. Considering the experimental bias in the determination of TTRs by the tangent method in DSC analyses, this temperature has been chosen in order to achieve the complete reverse martensitic transformation upon heating; moreover, the surface temperature of the samples has been continuously measured by using a K-type thermocouple to avoid reaching the T_g of PE resin. During the heating process, the wire tries to recover its initial pre-strain so that the PE resin capability of remaining well bonded to the SMA wire can be studied. Finally, the interfacial adhesion before and after the strain recovery tests has been investigated by means of electron microscopy.

RESULTS AND DISCUSSION

In general, a typical pull-out curve can be divided into two regions. The first is characterised by a pre-fracture straining of the interface, in which the applied load increases due to the deformation of the free length of the wire. The force increases until the interface fracture occurs, causing the wire inside the composite to slip. In some cases, the debonding generates a sudden drop in force close to zero, while in others the post-fracture region begins. In this second region the force can settle down into a lower fairly constant level or can rapidly oscillate around a mean value due to a stick-slip behaviour until the wire completely pulls out [32]. Many theoretical studies [37, 38, 41] showed that the NiTi-composite interface fails with a typical brittle process and that interfacial bonding can be evaluated following two different criteria. The first is based on the assumption that debonding occurs when the shear stress at the interface exceeds the interfacial shear resistance. The second one suggests that the crack initiates at the point of wire entry due to accumulated strain; then the crack propagates until the complete debonding of the interface, according to brittle fracture propagation theory.

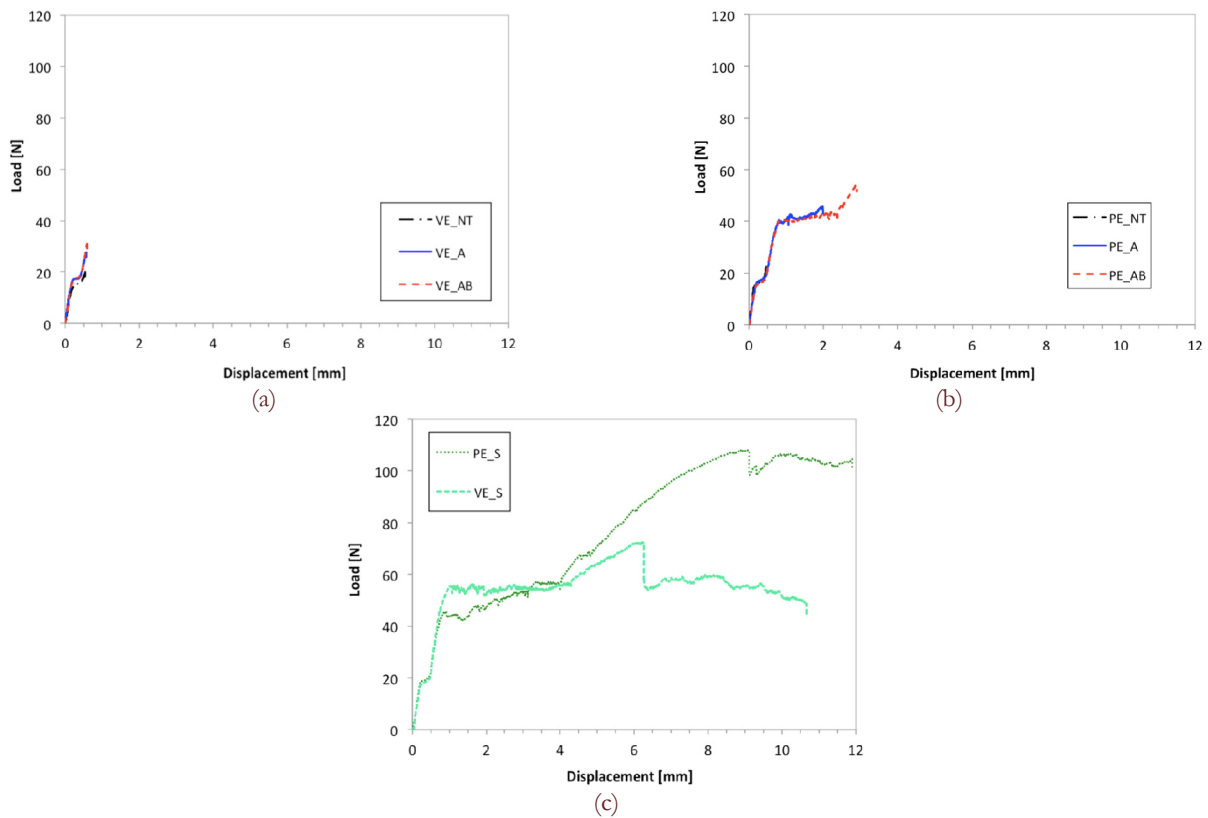


Figure 2: Pull-out curves for (a) VE_NT, VE_A and VE_AB samples, (b) PE_NT, PE_A and PE_AB samples, (c) VE_S and PE_S samples.

Fig. 2 depicts the results obtained from the pull-out tests performed on the samples, in which the NiTi wires subjected to different surface treatments are embedded in the two PE and VE resins. In particular, Fig. 2a shows the curves related to the pull-out samples realised with VE resin and in the surface conditions of the NT, A and AB wires. Fig. 2b shows the results of the pull-out tests for the PE resin with embedded wires in the NT, A and AB surface conditions. The pull-out curves of the samples in VE and PE resin with wires functionalised with the silane coupling agent are compared in Fig. 2c. In Fig. 2 it should be noted that the cutting-off of the pull-out curves corresponding to the sudden drop to the quasi-zero load level is marked with a short vertical solid line.

As can be seen, all curves present a small plateau of 0.2-0.3 mm in correspondence to an applied force of ≈ 15 -20 N. This plateau should be compared with the one observed in Fig. 3, which reports the engineering stress-strain curve of the same free heated NiTi wire. Therefore, in this initial region of the pull-out test the curve reproduces only the stress-strain behaviour of the free length wire.

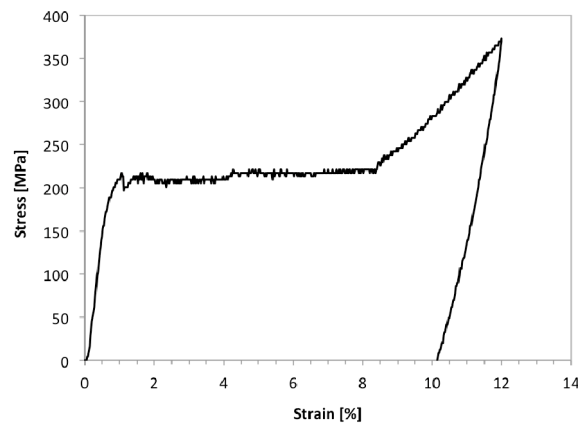


Figure 3: Engineering stress-strain curve for the heated NiTi wire.



In Fig. 2a it can be observed that the debonding suddenly occurs after less than 1 mm of displacement with a load value lower than the level necessary to produce the detwinning of the martensitic phase: the PE resin with a no surface-treatment wire embedded into it also shows the same behaviour (Fig. 2b). In contrast, after the small initial plateau in the PE_A and PE_AB samples the load further increases and reaches a level sufficient to induce the martensitic twinning rearrangement of the free length wire. This is in good agreement with the engineering stress-strain curve of the free wire previously heated in order to remove any pre-strain (Fig. 3). In the case of the PE_AB sample the load at which the interface failure occurs is greater than the load at which the phase transformation takes place.

The pull-out curves for the samples functionalised with the silane coupling agent (Fig. 2c) show that the load levels reached by the PE_E and VE_S samples after the martensitic plateau are greater than that reached by the PE_AB sample. Moreover, in all the other samples the force drops close to zero after the failure of the interface, while in the VE_S and PE_S samples the force suddenly drops and settles down to a lower value. Assuming that at this load level the wire starts to slip inside the composite, the applied load could now be related to the friction acting at the polymer/wire interface. For the PE_S sample this value is close to the peak load value, while for the VE_S sample the actual load level is similar to the detwinning plateau load.

By analysing the curves of Fig. 2b, but also of Fig. 2c, another alternative consideration can be drawn. The rise of the load after the detwinning plateau begins at a level of displacement lower than the onset of the elastic deformation of the detwinned martensite for the free wire ($\approx 8\%$). The increase in load starting at a level of displacement less than 8% could be justified considering that, after the detwinning of the free length of the wire, the detwinning of the embedded length is partially constrained by the polymeric matrix. In the case of the PE_A sample this could be an indication that interface failure occurs before the beginning of the martensitic reorientation of the embedded length of the wire because the adhesion is not strong enough to support the increase of the load.

Several approaches may be used to explain the peculiar patterns in Fig. 2. In agreement with [41, 42], analysis of the load-displacement curve enables two different interfacial failure mechanisms to be distinguished. When the interfacial failure occurs without friction acting on the interface, the load-displacement curve increases concave-up prior to the peak load values, corresponding to the interfacial fracture (all cases of Fig. 2a and PE_NT plus PE_AB in Fig. 2b). Moreover, the quasi-zero PFFP ("post-fractures friction pull-out") load levels should be a further indication that frictional shear forces do not act on the already debonded wire before the failure of the interface. Accordingly, when the frictional shear force acting on the already debonded wire is present, the load increases with a decreasing slope (concave-down) as it approaches the peak load values (PE_AB in Fig. 2b and all cases of Fig. 2c). However, it should be noted in Fig. 2c that in the case of PE_S samples the slope is smaller than the values collected for VE_S specimens and the PFFP load levels are close to the peak load value. Such behaviour could indicate much more mechanical interactions and not just friction between the NiTi wire and polymeric matrix. After debonding, particles of wire and/or resin may cause a wedging action that increases the interface friction; thus, the interfacial contact pressure increases which requires additional shrinkage of the wire to pull itself away from the matrix [41].

According to several authors [20, 23, 24] a more adequate approach to the description of the pull-out curves must take into account that several simultaneous processes occur in the specimens in the case of good adhesion (Fig. 2c). When large forces are applied to the wire, at least three regions can be considered at the interface: (i) the region where the tensile stress in the wire is small and phase transformation has still not occurred (far from the loaded wire end); (ii) the region in which phase transformation has just taken place (in the middle of the embedded wire length); (iii) the region in which phase transformation is already completed (near the loaded end). It can be noted that, taking into account the interfacial debonding in the pull-out process, the interfacial crack tip (depending on interfacial adhesion and applied load, it can be localised in any of these regions) and the already debonded regions with interfacial friction between the wire and the matrix should also be included.

With regards to the shapes of the "tails" in Fig. 2c, they can also be due to the fact that the phase transformation region moves along the interface. The difference between the two curves in Fig. 2c could result, in turn, from the fact that if the interfacial adhesion for the two specimens is different, then the size and location of the phase transformation regions may also be different. In particular, Chang et al. [43] demonstrated that at a relatively high loading rate or in a thermally insulating environment phase transformation involves several nucleation sites and more transformation fronts that will propagate away from one another.

The force levels for pulling the functionalised actuators out of the resins can provide useful information about the nature of the adhesion between the NiTi wires and the VE and PE polymeric matrices. Paine et al. [32] demonstrated that good wettability is a fundamental requirement for the chemical cohesion between the polymeric matrix and the surface of the actuator. Accordingly, the less viscous PE resin will be easily spread and wet the surface of the wire with a low contact angle. The highest peak load values exhibited by the functionalised wires (Fig. 2c) could also be related to the bridging



action caused by the silane coupling agent. The silane is able to covalently attach itself to both a metal oxide surface through a silicon-chlorine or silicon-methoxy bond and the propagating polymer chain. Smith et al. [36] proved that the chemical binding to the matrix rather than polymer chain entanglement is the cause of the roughly 100% relative increased adhesion and the higher shear stress strength.

Another way to enhance interfacial adhesion between the actuator and the resin is by physical adhesion through mechanical interaction. If the surface of the NiTi wire is made rougher by sandblasting or chemical etching, for example, a polymer of low viscosity can fill the crevices and form mechanical projection that hinders the pull-out of the wire. Fig. 4 shows SEM micrographs of the surfaces of the wires after the different surface treatment conditions. The SEM micrograph for the functionalised wires is not reported since the modification of the surface chemistry does not alter the surface topology of the constituent. Based on the peak load levels in Fig. 2a and b, the more viscous VE resin suffers in comparison with the PE resin in this aspect of adhesion as well.

For rough surfaces (Fig. 4b and c) the mechanical interaction with the polymeric matrix is increased as well as the interfacial adhesion and the peak load levels (VE_A, PE_A and much more VE_AB plus PE_AB in Fig. 2a and b); in contrast, for smooth surfaces (Fig. 4a), if poor mechanical interaction is present the bond strength is completely dependent on the intermolecular attraction based on hydrogen or Van der Waals bonds, which could be occurred [32].

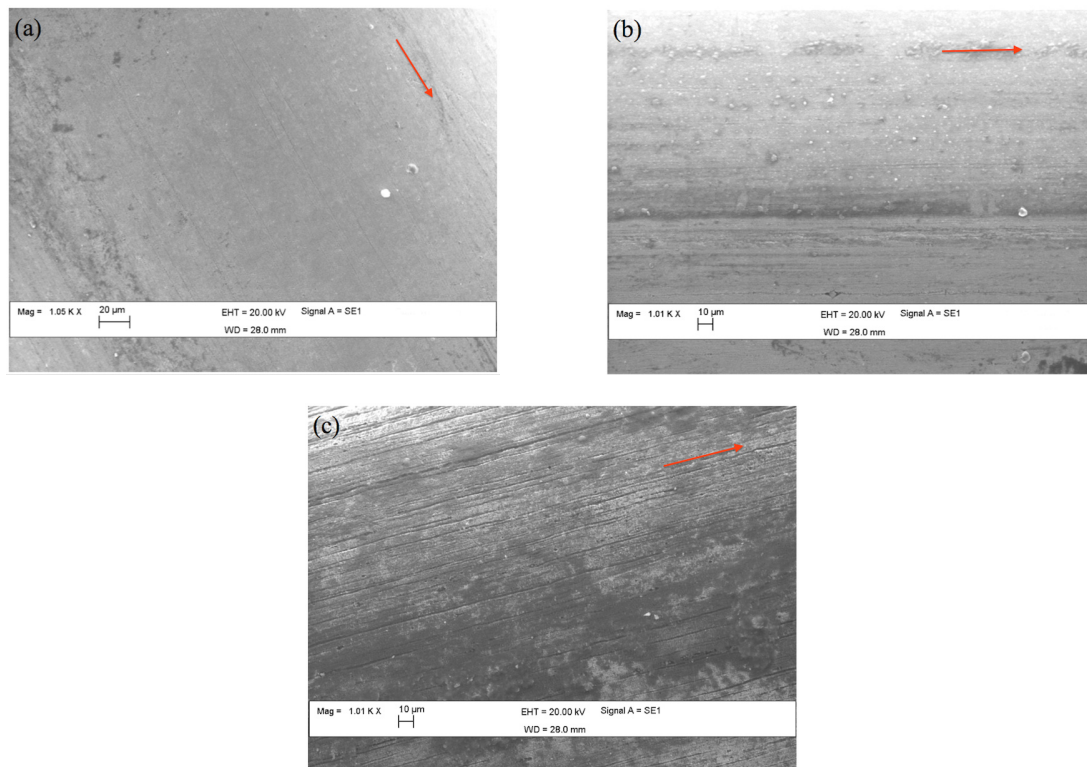


Figure 4: SEM micrographs of the surfaces of the wires for the different surface treatment conditions: (a) NT, (b) A and (c) AB samples, respectively. (Red arrow indicates the main direction of the wire).

For the same four different surface treatment conditions, the SEM analysis of the PE/wire interfaces before the strain recovery tests highlighted around a 10 μm -thick native oxide layer interposed between the polymer and metal surfaces (Fig. 5). In Fig. 5a the native oxide resulting from the oxidation reactions occurring during the heating of the wire is evident. According to Rossi et al. [44] the EDS analyses performed at the native oxide/metal alloy interface (yellow arrow in Fig. 5a) confirmed the titanium depletion in the outer surface of the alloy and the consequent nickel enrichment due to the outward migration of the titanium to form the oxide layer.

The increased roughness of the native oxide caused by the chemical etching treatments should be noted in Fig. 5b and c. The SEM observations are consistent with the demonstrated improvement in both physical adhesion and interfacial adhesion due to the mechanical interaction between the wire and the polymer matrix. It is well known that native oxides usually enhance the interfacial adhesion because of their higher roughness; however, several studies highlighted that they

may also show two drawbacks: reduction of the NiTi alloy volume that displays shape memory effect and debonding from the matrix when the de-cohesive failure of the oxide occurs [44, 45]. As previously highlighted, the modification of the surface chemistry does not alter the surface topology of the wire. Accordingly, the SEM micrograph for the wire functionalised with the silane coupling agent is not reported since the appearance of the PE/wire interface is comparable to the PE/wire interface observed for the untreated sample.

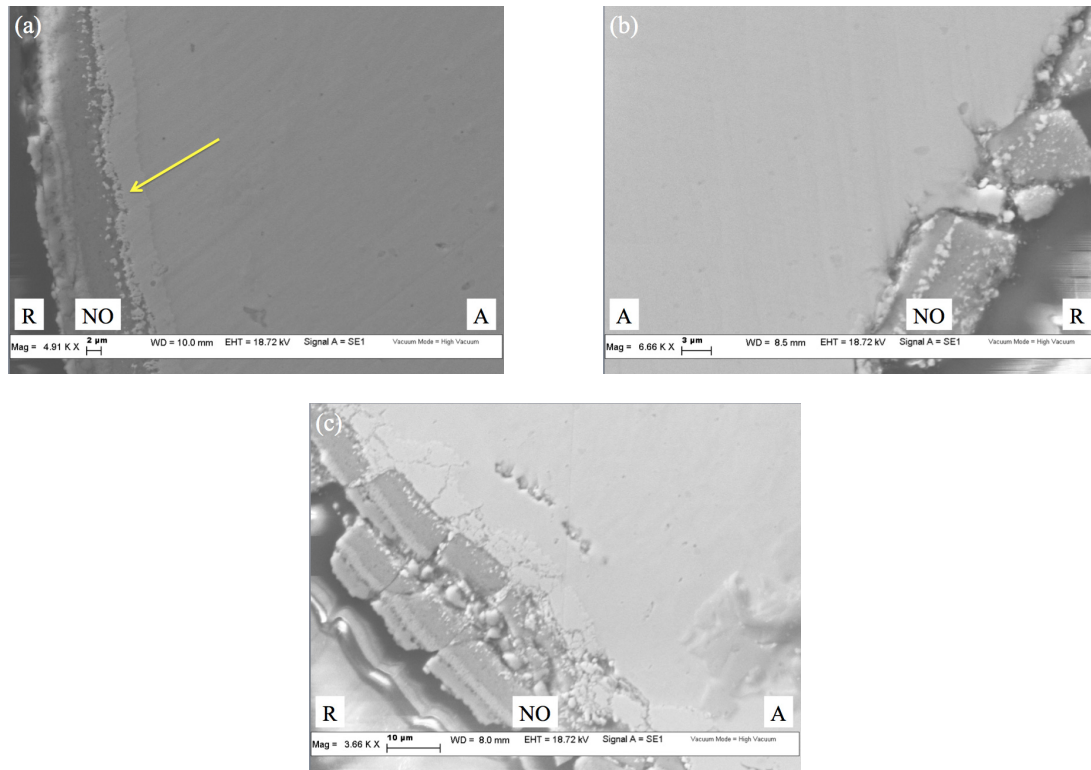


Figure 5: SEM micrographs of the PE/wire interfaces before the strain recovery tests: (a) NT, (b) A and (c) AB samples, respectively. (R = resin, NO = native oxide and A = alloy).

With regard to the interfacial adhesion after the strain recovery tests, the debonding of the wires pre-strained at 5% and 6% are observed for all the polymer/wire interfaces considered. The strain recovery action of the embedded wires produces high interfacial stresses that cause debonding at the end of the bonded region. No evidence of radial cracks in the polymeric matrix is observed. Similarly, debonding occurs for the wires pre-strained at 4% whether or not they were chemical treated. At this pre-strain level both untreated and etched in the 40% HNO_3 water solution, wires do not show the development of radial cracking on the resin surface (Fig. 6a). Conversely, some cracks appear at the polymer/wire interface in samples with wires etched in the 5% HNO_3 + 15% HF water solution (Fig. 6b). For the functionalised wires, even if the wire is debonded from the matrix, many radial cracks are evident (Fig. 6c), meaning it is the highest stress transfer between wire and matrix when compared to the previous surface treatment conditions. Several authors [13, 46, 47] have demonstrated that the development of radial shear cracks is related to the residual stresses caused by thermal cycling. Moreover, stresses acting at the interface are strongly dependent on the phase transformation that occurs during heating above A_f and the subsequent cooling down. The thermal mismatch between the embedded SMA wire and the surrounding matrix produces high tensile stresses at the end of the bonded region that can lead to the matrix cracking in the radial direction. The higher the pre-strain level, the heavier the stress will be. However, lower magnitude of the increasing stress is reported in the case of an SMA wire embedded in carbon or Kevlar composites, since these functional structures give negative thermal strain with increasing temperature. Finally, it can be demonstrated that the use of PE resin in a smart composite may produce an increase of 60% in the tensile stress at the beginning of the recovery thanks to the increased thermal expansion coefficient of polyester [46].

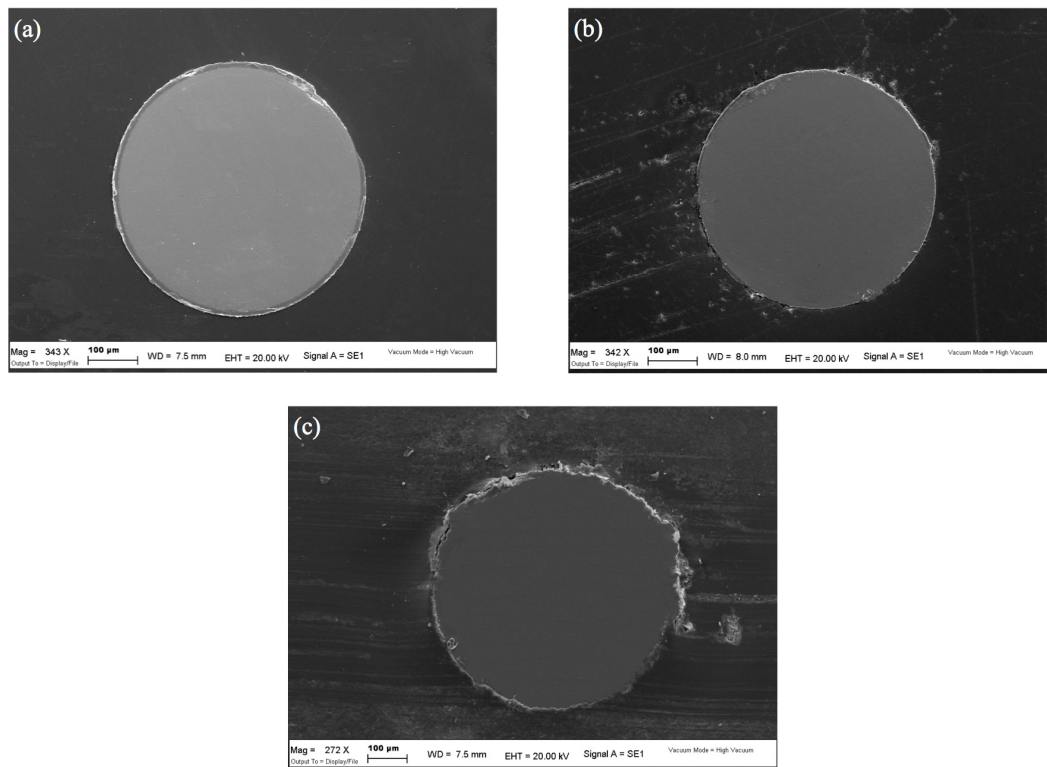


Figure 6: SEM micrographs of the PE/wire interfaces after the strain recovery tests for wires pre-strained at 4%. (a) A and (b) AB samples, respectively; (c) wire functionalised with the silane coupling agent.

CONCLUSIONS

Based on the results obtained regarding improved adhesion of NiTi wires embedded in PolyEster (PE) and VinylEster (VE) resins, the following conclusions can be drawn:

- Pull-out tests prove the better adhesion between the NiTi wires and the PE resin. The highest interfacial adhesion is obtained by the functionalisation of the surfaces of the wires with a silane coupling agent.
- The physical adhesion between the PE resin and both untreated and chemical etched wires is confirmed. In particular, it is demonstrated by electron microscopy analysis that the adhesion is a result of mechanical interactions due to the increased roughness of the native oxide caused by the chemical etching treatments. Conversely, for the functionalised wires chemical adhesion is promoted by the chemical binding of the silane to the resin. Cohesion is also enhanced by the good wettability between the polymeric matrix and the surface of the actuator.
- The strain recovery tests indicate early debonding of the wires pre-strained at 5% and 6% for all the PE/wire interfaces considered. In the case of wires pre-strained at 4%, radial shear cracks on the resin surface are observed by SEM for wires both functionalised and etched in a 5% HNO_3 + 15% HF water solution. The thermal mismatch between the embedded SMA wire and the surrounding matrix produces high tensile stress at the end of the bonded region that can lead to the matrix cracking in the radial direction.

REFERENCES

- [1] Otsuka, K., Wayman, C.M., *Shape Memory Materials*, Cambridge University Press, Cambridge, (1998).
- [2] Lagoudas, D.C., Tadjbakhsh, I.G., *Active flexible rods with embedded SMA fibers*, *Smart Mater. Struct.*, 1 (1992) 162-167.



- [3] Rocher, P., El Medawa, L., Hornez, J.-C., Traisnel, M., Breme, J., Hildebrand, H.F., Biocorrosion and cytocompatibility assessment of NiTi shape memory alloys, *Scripta Mater.*, 50 (2004) 255-260.
- [4] Chen, M.F., Yang, X.J., Liu, Y., Zhu, S.L., Cui, Z.D., Man, H.C., Study on the formation of an apatite layer on NiTi shape memory alloy using a chemical treatment method, *Surf. Coat. Tech.*, 173 (2003) 229-234.
- [5] Trigwell, S., Hayden, R.D., Nelson, K.F., Selvaduray, G., Effects of surface treatment on the surface chemistry of NiTi alloy for biomedical applications, *Surf. Interface Anal.*, 26 (1998) 483-489.
- [6] Wei, Z.G., Sandström, R., Miyazaki, S., Review. Shape-memory materials and hybrid composites for smart systems. Part I Shape-memory materials, *J. Mater. Sci.*, 33 (1998) 3743-3762.
- [7] Wei, Z.G., Sandström, R., Miyazaki, S., Review. Shape-memory materials and hybrid composites for smart systems. Part II Shape-memory hybrid composites, *J. Mater. Sci.*, 33 (1998) 3763-3783.
- [8] Hebda, D.A., Whitlock, M.E., Ditman, J.B., White, S.R., Manufacturing of adaptive graphite/epoxy structures with embedded Nitinol wires, *J. Intel. Mat. Syst. Str.*, 6 (1995) 220-228.
- [9] Tsoi, K.A., Stalmans, R., Schrooten, J., Transformational behaviour of constrained shape memory alloys, *Acta Mater.*, 50 (2002) 3535-3544.
- [10] Jang, B.K., Kishi, T., Adhesive strength between TiNi fibers embedded in CFRP composites, *Mater. Lett.*, 59 (2005) 1338-1341.
- [11] Kim, C., A smart polymer composite actuator with thin SMA strips, *Int. J. Mod. Phys. B*, 20 (2006) 3733-3738.
- [12] Murasawa, G., Tohgo, K., Ishii, H., Deformation behavior of NiTi/polymer shape memory alloy composites - experimental verifications, *J. Compos. Mater.*, 38 (2004) 399-416.
- [13] Lau, K.-T., Chan, A.W.-L., Shi, S.-Q., Zhou, L.M., Debond induced by strain recovery of an embedded NiTi wire at a NiTi-epoxy interface: micro-scale observation, *Mater. Des.*, 23 (2002) 265-270.
- [14] Merlin, M., Soffritti, C., Fortini, A., Study of the heat treatment of NiTi shape memory alloy strips for the realisation of adaptive deformable structures, *Metallurgia Italiana*, 103 (2011) 17-21.
- [15] Rizzoni, R., Merlin, M., Casari, D., Shape recovery behaviour of NiTi strips in bending: Experiments and modelling, *Cont. Mech. Therm.*, 25 (2013) 207-227.
- [16] Tahiri, V.-L., Patoor, E., Eberhardt, A., An analysis of the thermomechanical behaviour of a shape memory alloy/elastomer composite, *J. Phys. IV*, 115 (2004) 195-203.
- [17] Winzek, B., Sterzl, T., Rumpf, H., Quandt, E., Composites of different shape memory alloys and polymers for complex actuator motions, *J. Phys. IV*, 112 (2003) 1163-1168.
- [18] Barrett, R., Gross, R.S., Super-active shape-memory alloy composites, *Smart Mater. Struct.*, 5 (1996) 255-260.
- [19] James, G.B., Lagoudas, D.C., Thermomechanical response of shape memory composites, *J. Intel. Mat. Syst. Str.*, 5 (1994) 333-346.
- [20] Wang, X., Hu, G., Stress transfer for a SMA fibre pulled out from an elastic matrix and related bridging effect, *Compos. Part A-Appl. Sci. Manuf.*, 36 (2005) 1142-1151.
- [21] Liu, P.F., Yu, X.Z., Guo, Y.M., Tao, W.M., Interface debonding criteria in SiC fiber-reinforced composites, *J. Zhejiang Univ. (Eng. Sci.)*, 40 (2006) 1883-1888.
- [22] Hsueh, C.-H., Stress transfer from axially loaded fiber to matrix in a microcomposite, in: *Proceedings of Materials Research Society Symposium*, Pittsburgh, (1995) 217-227.
- [23] Wang, Y., Zhou, L., Wang, Z., Huang, H., Ye, L., Stress distributions in single shape memory alloy fiber composites, *Mater. Design*, 32 (2011) 3783-3789.
- [24] Wang, Y., Zhou, L., Wang, Z., Huang, H., Ye, L., Analysis of internal stresses induced by strain recovery in a single SMA fiber-matrix composite, *Compos. Part B-Eng.*, 42 (2011) 1135-1143.
- [25] Man, H.C., Ho, K.L., Cui, Z.D., Laser surface alloying of NiTi shape memory alloy with Mo for hardness improvement and reduction of Ni²⁺ ion release, *Surf. Coat. Tech.*, 200 (2006) 4612-4618.
- [26] Cui, Z.D., Man, H.C., Yang, X.J., The corrosion and nickel release behavior of laser surface-melted NiTi shape memory alloy in Hanks' solution, *Surf. Coat. Tech.*, 192 (2005) 347-353.
- [27] Villiermaux, F., Tabrizian, M., Yahia, L'H., Meunier, M., Piron, D.L., Excimer laser treatment of NiTi shape memory alloy biomaterials, *Appl. Surf. Sci.*, 109-110 (1997) 62-66.
- [28] Cui, Z.D., Man, H.C., Yang, X.J., Characterization of the laser gas nitrided surface of NiTi shape memory alloy, *Appl. Surf. Sci.*, 208-209 (2003) 388-393.
- [29] Man, H.C., Zhao, N.Q., Phase transformation characteristics of laser gas nitrided NiTi shape memory alloy, *Surf. Coat. Tech.*, 200 (2006) 5598-5605.
- [30] Man, H.C., Zhao, N.Q., Enhancing the adhesive bonding strength of NiTi shape memory alloys by laser gas nitriding and selective etching, *Appl. Surf. Sci.*, 253 (2006) 1595-1600.



- [31] Jonnalagadda, K., Kline, G.E., Sottos, N.R., Local displacements and load transfer in shape memory alloy composites, *Exp. Mech.*, 37 (1997) 78-86.
- [32] Paine, J.S.N., Jones, W.M., Rogers, C.A., Nitinol actuator to host composite interfacial adhesion in adaptive hybrid composites, in: *Proceedings of 33rd Structures, Structural Dynamics and Materials Conference*, Dallas, (1992) 556-565.
- [33] Ju, X., Dong, H., Plasma surface modification of NiTi shape memory alloy, *Surf. Coat. Tech.*, 201 (2006) 1542-1547.
- [34] Poon, R.W.Y., Yeung, K.W.K., Liu, X.Y., Chu, P.K., Chung, C.Y., Lu, W.W., Cheung, K.M.C., Chan, D., Carbon plasma immersion ion implantation of nickel-titanium shape memory alloys, *Biomaterials*, 26 (2005) 2265-2272.
- [35] Neuking, K., Abu-Zarifa, A., Eggeler, G., Surface engineering of shape memory alloy/polymer-composites: improvement of the adhesion between polymers and pseudoelastic shape memory alloys, *Mater. Sci. Eng. A*, 481-482 (2008) 606-611.
- [36] Smith, N.A., Antoun, G.G., Ellis, A.B., Crone, W.C., Improved adhesion between nickel-titanium shape memory alloy and a polymer matrix via silane coupling agents, *Compos. Part A-Appl. Sci. Manuf.* 35 (2004) 1307-1312.
- [37] Zhou, L.-M., Kim, J.-K., Mai, Y.-W., Interfacial debonding and fibre pull-out stresses. Part II A new model based on the fracture mechanics approach, *J. Mater. Sci.*, 27 (1992) 3155-3166.
- [38] Zhou, L.-M., Mai, Y.-W., Baillie, C., Interfacial debonding and fiber pull-out stresses. Part V A methodology for evaluation of interfacial properties, *J. Mater. Sci.*, 29 (1994) 5541-5550.
- [39] Fu, S.-Y., Yue, C.-Y., Hu, X., Mai, Y.W., Analyses of the micromechanics of stress transfer in single-and multi-fibre pull-out tests, *Compos. Sci. Technol.*, 60 (2000) 569-579.
- [40] Poon, C.K., Zhou, L.M., Jin, W., Shi, S.Q., Interfacial debond of SMA composites, *Smart Mater. Struct.*, 14 (2004) 29-37.
- [41] Paine, J.S.N., Rogers, C.A., Characterization of interfacial shear strength between SMA actuators and host composite material in adaptive composite material systems, in: *Adaptive Structures and Material Systems ASME*, AD-35, New York, (1993) 63-70.
- [42] Piggott, M.R., Failure processes in the fibre-polymer interphase, *Compos. Sci. Technol.*, 42 (1991) 57-76.
- [43] Chang, B.-C., Shaw, J.-A., Iadicola, M.A., Thermodynamics of shape memory alloy wire: modeling, experiments, and application, *Continuum Mech. Thermodyn.*, 18 (2006) 83-118.
- [44] Rossi, S., Deflorian, F., Pegoretti, A., D'Orazio, D., Gialanella, S., Chemical and mechanical treatments to improve the surface properties of shape memory NiTi wires, *Surf. Coat. Tech.*, 202 (2008) 2214-2222.
- [45] Kinloch, A.J., *Adhesion and Adhesives: Science and Technology*, Chapman & Hall, London, (1987).
- [46] Berman, J.B., White, S.R., Theoretical modelling of residual and transformational stresses in SMA composites, *Smart Mater. Struct.*, 5 (1996) 731-743.
- [47] Poon, C.-K., Lau, K.-T., Zhou, L.-M., Design of pull-out stresses for prestrained SMA wire/polymer hybrid composites, *Compos. Part B-Eng.*, 36 (2005) 25-31.